THE GERONTOLOGICAL SOCIETY OF AMERICA®

Journals of Gerontology: Biological Sciences
cite as: *J Gerontol A Biol Sci Med Sci*, 2018, Vol. 73, No. 7, 853–863
doi:10.1093/gerona/glx177
Advance Access publication October 7, 2017

OXFORD

Original Article

Nrf2 Deficiency Exacerbates Obesity-Induced Oxidative Stress, Neurovascular Dysfunction, Blood–Brain Barrier Disruption, Neuroinflammation, Amyloidogenic Gene Expression, and Cognitive Decline in Mice, Mimicking the Aging Phenotype

Stefano Tarantini, PhD,[1,2,*] M. Noa Valcarcel-Ares, PhD,[1,*] Andriy Yabluchanskiy, MD, PhD,[1,2,*] Zsuzsanna Tucsek, PhD,[1,*] Peter Hertelendy, MD,[1,3,*] Tamas Kiss, MD,[1,3] Tripti Gautam, MS,[1] Xin A. Zhang, MD, PhD,[4,5] William E. Sonntag, PhD,[1,2] Rafael de Cabo, PhD,[6] Eszter Farkas, PhD,[3] Michael H. Elliott, PhD,[7,8,9] Michael T. Kinter, PhD,[10] Ferenc Deak, MD, PhD,[1,7,11] Zoltan Ungvari, MD, PhD,[1,2,3,4,5,7] and Anna Csiszar, MD, PhD[1,2,3,4,5,7]

[1]Reynolds Oklahoma Center on Aging, Department of Geriatric Medicine and [2]Translational Geroscience Laboratory, Department of Geriatric Medicine, University of Oklahoma Health Sciences Center, Oklahoma City. [3]Department of Medical Physics and Informatics, Faculty of Medicine and Faculty of Science and Informatics, University of Szeged, Hungary. [4]Department of Physiology and [5]Peggy & Charles Stephenson Oklahoma Cancer Center, University of Oklahoma Health Sciences Center, Oklahoma City. [6]Translational Gerontology Branch, National Institute on Aging, Baltimore, Maryland. [7]Oklahoma Center for Neuroscience, [8]Department of Ophthalmology, and [9]Dean McGee Eye Institute, University of Oklahoma Health Sciences Center, Oklahoma City. [10]Aging and Metabolism Research Program, Oklahoma Medical Research Foundation, Oklahoma City. [11]Harold Hamm Diabetes Center, University of Oklahoma Health Sciences Center, Oklahoma City.

*These authors contributed equally to this work.

Address correspondence to: Anna Csiszar, MD, PhD, Reynolds Oklahoma Center on Aging, Department of Geriatric Medicine, University of Oklahoma HSC, 975 N. E. 10th Street, Oklahoma City, OK 73104. E-mail: anna-csiszar@ouhsc.edu

Received: May 25, 2017; Editorial Decision Date: September 3, 2017

Decision Editor: Rozalyn Anderson, PhD

Abstract

Obesity has deleterious effects on cognitive function in the elderly adults. In mice, aging exacerbates obesity-induced oxidative stress, microvascular dysfunction, blood–brain barrier (BBB) disruption, and neuroinflammation, which compromise cognitive health. However, the specific mechanisms through which aging and obesity interact to remain elusive. Previously, we have shown that Nrf2 signaling plays a critical role in microvascular resilience to obesity and that aging is associated with progressive Nrf2 dysfunction, promoting microvascular impairment. To test the hypothesis that Nrf2 deficiency exacerbates cerebromicrovascular dysfunction induced by obesity $Nrf2^{+/+}$ and $Nrf2^{-/-}$, mice were fed an adipogenic high-fat diet (HFD). Nrf2 deficiency significantly exacerbated HFD-induced oxidative stress and cellular senescence, impairment of neurovascular coupling responses, BBB disruption, and microglia activation, mimicking the aging phenotype. Obesity in $Nrf2^{-/-}$ mice elicited complex alterations in the amyloidogenic gene expression profile, including upregulation of amyloid precursor protein. Nrf2 deficiency and obesity additively reduced long-term potentiation in the CA1 area of the hippocampus. Collectively, Nrf2 dysfunction exacerbates the deleterious effects of obesity, compromising cerebromicrovascular and brain health by impairing neurovascular coupling mechanisms, BBB

integrity and synaptic function and promoting neuroinflammation. These results support a possible role for age-related Nrf2 dysfunction in the pathogenesis of vascular cognitive impairment and Alzheimer's disease.

Keywords: Vascular cognitive impairment, Vascular cognitive impairment, Long-term potentiation, Vascular contributions to cognitive impairment and dementia, Endothelial dysfunction

Currently, close to 70% of Americans aged 65 years and over are overweight and over 35% are obese and it is predicted that nearly half of the elderly population in the United States will be obese by 2030. Epidemiological and clinical studies, including the Framingham Offspring Study, demonstrate that a negative correlation exists between adiposity and cognitive function and that the deleterious effects of obesity on higher cortical function are exacerbated in the elderly adults (1–4). Common mechanisms that contribute to the effects of aging and obesity are hypothesized to increase susceptibility to both vascular cognitive impairment (VCI) and neurodegeneration, including Alzheimer's disease.

There is an increasing appreciation that alterations at the level of the cerebral microcirculation play a key role in the pathogenesis of both VCI and Alzheimer's disease (AD) in elderly patients (5,6). Preclinical studies provide direct mechanistic evidence that advanced age and obesity have multifaceted synergistic effects compromising cerebromicrovascular health (7–10), which are causally linked to cognitive decline.

Normal functioning of the central nervous system requires a continuous, tightly-controlled supply of oxygen and nutrients as well as washout of harmful metabolites through uninterrupted cerebral blood flow (CBF) (5). During periods of intense neuronal activity, there is a requirement for rapid adaptive increases in CBF, which is ensured by a mechanism known as neurovascular coupling. Impairment of neurovascular coupling responses has been causally linked to cognitive decline (11). Previous studies demonstrate that obesity results in neurovascular uncoupling, which is markedly exacerbated at old age (8). Although the available clinical and preclinical data suggest that advanced age and obesity have synergistic vascular effects (7–9), there are no studies addressing the specific age-related mechanisms through which aging exacerbates obesity-induced neurovascular uncoupling.

There is also increasing evidence to support an essential role for factors that compromise the integrity of the blood–brain barrier (BBB) in the onset and progression of both VCI and Alzheimer's disease (12), by triggering neuroinflammation, synaptic dysfunction, and neurodegeneration. Experimental and clinical studies suggest that obesity promotes BBB breakdown and activates inflammatory processes, which contribute to obesity-related impairment of cognitive function (13,14). Importantly, aging was shown to exacerbate obesity-induced BBB disruption and neuroinflammation (7), yet, the underlying mechanisms remain obscure.

NF-E2-related factor 2 (Nrf2) is an evolutionarily highly conserved pro-survival transcription factor that upregulates the expression of numerous genes involved in cellular resilience including enzymes that detoxify reactive oxygen species (ROS), as well as those with other antioxidant properties (15–19). In young organisms, Nrf2-driven pathways attenuate vascular oxidative stress and limit the damage caused by the increased production of ROS induced by obesity (18,19). Previously, we have demonstrated that aging is associated with Nrf2 dysfunction in the vasculature, which was proposed to increase sensitivity of aged organisms to oxidative stress-induced vascular damage (20,21). Further, indirect evidence raises the possibility that impaired Nrf2 signaling and increased cerebral oxidative stress may contribute to obesity-induced declines in cognitive performance in the aged brain (22).

The present study was designed to directly test the hypothesis that Nrf2 deficiency exacerbates obesity-induced neurovascular dysfunction, BBB disruption, neuroinflammation, and synaptic dysfunction in the hippocampus, mimicking the aging phenotype. To test our hypothesis, we assessed changes in whisker stimulation-induced functional hyperaemia in the somatosensory cortex, BBB function, microglia activation, hippocampal cytokine expression, and markers of oxidative stress in high-fat diet-fed obese Nrf2 deficient ($Nrf2^{-/-}$) and wild type mice. To determine whether enhanced neuroinflammation triggers early processes involved in the development of VCI and/or AD, we also studied long-term potentiation (LTP) and hippocampal expression of genes involved in regulation of the cellular amyloid precursor protein (APP)-dependent signaling pathways, β-amyloid generation and the pathogenesis of tauopathy.

Methods

Experimental Animals, High-fat Diet Feeding

Male WT mice ($Nrf2^{+/+}$) and Nrf2 KO mice on an Institute of Cancer Research (ICR) background ($Nrf2^{-/-}$) were used as reported previously (16–18). In this study, only male mice were studied to exclude the possible confounding effects of the estrous cycle in females. The mice were housed in an environmentally-controlled vivarium with unlimited access to water and a controlled photoperiod (12-hour light; 12-hour dark). Body weight was recorded biweekly. All mice were maintained according to National Institutes of Health guidelines and all animal use protocols were approved by the Institutional Animal Care and Use Committees of the participating institutions. At 3 months of age, both wild-type control and $Nrf2^{-/-}$ mice were assigned to two groups and were fed a standard D12492 diet (SD; 10% kcal from fat) or D12450B diet modified to provide 60% of calories from fat (high-fat diet; HFD; Research Diets Inc., New Brunswick, NJ), as described previously (23). The animals continued on the specific diets (with water and food ad libitum) for 5 months. There was considerable variation in the initial body weight (41 ± 2 g and 36 ± 2 g for $Nrf2^{+/+}$ and $Nrf2^{-/-}$ mice, respectively) and HFD-induced weight gain in the mice and the intent of the studies was to determine the influence of HFD and Nrf2 on cerebromicrovascular health, independent of body weight gain differences. Therefore, we selected a cohort of mice from the larger population with a similar HFD-induced gain in mean body weight (≥20%), which indicates that results in Figures 1–4 are independent of body weight gain differences. An inherited retinal defect leading to rapid degeneration of photoreceptor cells is known to develop in ICR mice that are homozygous for a recessive mutation in the *Pdeb*^{rd1} gene (24). As impaired vision confounds the effects of behavioral studies, we screened the animals for the presence of this mutation in their genome and excluded homozygous carriers (n = 3) from the behavioral studies.

Serum Biomarkers

Whole blood was collected at sacrifice and was centrifuged at 2,500 x g for 20 minutes at 4°C; serum was collected, aliquoted, and stored at

–80°C. Blood glucose was determined using an Ascensia Elite glucose meter (Bayer, Mishawaka, IN). The serum biochemical profile was assessed by Vance Veterinary Laboratories (Oklahoma City, OK). Circulating levels of cytokines, chemokines, and other inflammatory markers relevant for aging research (7–9,23,25) were analyzed using a magnetic bead-based multiplex protein array system (EMD Millipore) according to the manufacturer's protocol.

Novel Object Recognition test

After 5 months on the HFD, the novel object recognition task was performed to characterize the effect of obesity on learning and memory (11,26). The results of the test are influenced by both hippocampal and cortical impairment. The test consists of a habituation phase, acquisition (familiarization) phase, and trial phase. During the habituation phase, the animals explored the empty open-field arena for 5 minutes. Then, in the acquisition phase, the mice explore two identical objects for 2 minutes. After a 4-hour delay, a trial phase occurred. During this period, animals explored the familiar object and a novel object for 2 minutes. Exploration of the objects was defined as directing the nose at a distance ≤2 cm to the object and/or touching it with the nose. For data collection and analysis, Ethovision software (Noldus Information Technology Inc., Leesburg, VA) was used. Sitting or climbing on it was not considered as an exploration. All objects used in this study were made of washable odorless plastic and were different in shapes and colors but identical in size. A percent of time spent exploring the novel object relative to the total time spent exploring both objects was used as a measure of novel object recognition. The Recognition Index (representing the time spent investigating the novel object [T_{novel}] relative to the total object investigation) was used as the main index of retention, which was calculated according to the following formula: (Recognition Index = $T_{novel}/[T_{novel} + T_{familiar}]$). The arena and the objects were cleaned with 70% ethanol between the trials to prevent the existence of olfactory cues.

Determination of Hippocampal Protein Carbonyl Content

As biomarkers of oxidative stress, protein carbonyl groups were quantified in cortical samples using the Protein Carbonyl Colorimetric Assay (Cayman Chemicals), following the manufacturer's protocol.

Measurement of Neurovascular Coupling Responses

After behavioral testing, neurovascular coupling responses in the whisker barrel cortex elicited by contralateral whisker stimulation were assessed in anesthetized mice, as previously described (8,11,27–30). In brief, mice in each group were anesthetized (α-chloralose (50 mg/kg, i.p.)/urethane (750 mg/kg, i.p.), endotracheally intubated and ventilated (MousVent G500; Kent Scientific Co, Torrington, CT). A thermostatic heating pad (Kent Scientific Co, Torrington, CT) was used to maintain rectal temperature at 37°C. End-tidal CO_2 (including dead space) was controlled between 3.2% and 3.7% to keep blood gas values within the physiologic range. Arterial blood pressure was monitored throughout the experiment with a noninvasive blood pressure monitor (CODA Monitor; Kent Scientific Co). The blood pressure was within the physiologic range throughout the experiments (90–110 mm Hg). Mice were immobilized, placed on a stereotaxic frame (Leica Microsystems Inc, Buffalo Grove, IL), the scalp and periosteum were pulled aside. The animals were equipped with an open cranial window as described (29) and a glass-insulated tungsten microelectrode (impedance, 2–3 MΩ, Kation Scientific, LLC, Minneapolis, MN) was inserted stereotaxically into the left barrel cortex (3 mm lateral and 1.5 mm caudal to bregma; depth of 0.6 mm) through the ACSF-perfused open cranial window for recording local field potentials. An Ag/AgCl electrode inserted in the neck muscles served as reference electrode. Changes in cerebral blood flow (CBF) were assessed above the left barrel cortex using a laser Doppler probe (Transonic Systems Inc., Ithaca, NY) as described (29). The right whisker pad was stimulated by a bipolar stimulating electrode placed to the ramus infraorbitalis of the trigeminal nerve and into the masticatory muscles. The stimulation protocol used to investigate NVC and somatosensory evoked field potentials consisted of 3 stimulation trials with an intertrial interval of 60 seconds, each delivering a 30-second train of electrical pulses (5 Hz, 1 mA, intensity, and 0.3 ms pulse width) to the mystacial pad. Changes in CBF were averaged and expressed as percent (%) increase from the baseline value. The electrical signal was amplified with a AC/DC differential amplifier (high pass at 1Hz, low pass at 1kHz) (Model 3000, A-M Systems, Inc. Carlsborg, WA), and digitalized by the PowerLab/Labchart data acquisition system (AD Instruments, Colorado Springs, CO) with the sampling rate of 40 kHz. The negative amplitude in the somatosensory evoked field potential response was considered as the field excitatory postsynaptic potential (fEPSP) (31). Experiments lasted ~30–40 minutes/mouse, which permitted stable physiological parameters to be obtained. The experimenter was blinded to the treatment of the animals.

Quantitative Real-Time RT-PCR

A quantitative real time RT-PCR technique was used to analyze mRNA expression of Nrf2 target genes (*Cat, Sod3, Hmox1, Mgst2, Gclc*), genes relevant for neurovascular dysfunction (including endothelial nitric oxide synthase [eNOS/*Nos3*], arginase [*Arg1*], $gp91^{phox}$ catalytic subunit of NADPH oxidase [*Cybb*], cyclooxygenase [*Ptgs1*], EET producing epoxygenases, and EET degrading soluble epoxide hydrolase [*Ephx2*]), senescence markers ($p16^{Ink4A}$/cyclin-dependent kinase inhibitor 2A/ *Cdkn2a*) and genes known to be involved in β-amyloid generation and Alzheimer's disease using validated TaqMan probes (Applied Biosystems) and a Strategen MX3000 platform, as previously reported (7,8,26). In brief, total RNA was isolated from cortical and hippocampal samples from each experimental group with a Mini RNA Isolation Kit (Zymo Research, Orange, CA) and was reverse transcribed using Superscript III RT (Invitrogen) (32,33). Quantification was performed using the efficiency-corrected ΔΔCq method. The relative quantities of the reference genes *Hprt1, Gapdh, Actb* and 18S were determined and a normalization factor was calculated based on the geometric mean for internal normalization. Fidelity of the PCR reaction was determined by melting temperature analysis and visualization of the product on a 2% agarose gel.

Quantitative Mass Spectrometry Analysis

Selective reaction monitoring mass spectrometry was used to quantify Nrf2-dependent antioxidant protein expression in cortical samples as previously described (34). For these assays, 60-μg amounts of tissue lysates were mixed with 8 pmol of bovine serum albumin (BSA) as an internal standard and 50 μL of 10% SDS. The samples were heated at 80°C for 15 minutes before precipitating the proteins in 80% acetone overnight at –20°C. The protein pellet was dissolved in 60 μL of sample buffer and a 20-μL aliquot containing

20 µg of protein run 1.5 cm into a 12.5% SDS-polyacrylamide gel. The gel was fixed and stained with GelCode Blue (Pierce). For each sample, the entire 1.5-cm lane was cut out of the gel and divided coarsely. The gel pieces were washed to remove the stain, reduced with DTT, alkylated with iodoacetamide, and digested with 1 µg of trypsin overnight at room temperature. The peptides produced in the digest were extracted with 50% methanol, 10% formic acid in water. The extract was evaporated to dryness and reconstituted in 150 µL of 1% acetic acid in water for analysis. The samples were analyzed using selective reaction monitoring with a triple quadrupole mass spectrometer (ThermoScientific TSQ Vantage) configured with a splitless capillary column HPLC system (Eksigent, Dublin, CA). Samples (10 µL) were injected onto a 10 cm × 75 µm C18 capillary column (Phenomenex, Jupiter C18). The column was eluted at 160 nL/min with a 30-minute linear gradient of acetonitrile in 0.1% formic acid. Data were processed by using Pinpoint to find and integrate the correct peptide chromatographic peaks. The response for each protein was taken as the total response for all peptides monitored. To quantify protein expression, the relative abundance of each protein was first normalized to the BSA internal standard and then normalized to the geometric mean of cellular reference proteins (34).

Western Blotting

To assess BBB integrity immunoblotting studies for extravasated IgG in hippocampal homogenates were performed. In brief, hippocampal samples (n = 4–6 per experimental group) from mice transcardially perfused with ice-cold PBS were homogenized in ice-cold phosphate buffered saline (PBS) with 1:100 Protease Inhibitor Cocktail (Sigma Aldrich). Samples were then subjected to SDS-PAGE gel electrophoresis and transferred to a nitrocellulose membrane. Membranes were blocked with 5% BSA (in 2% Tween in PBS, for 2 hours, at room temperature) and incubated with a primary antibody directed against IgG (sheep anti-mouse IgG, peroxidase-linked whole antibody, 1:500, at room temperature, Amersham NXA931) and then incubated with a appropriate HRP-conjugated secondary antibody (for 2 hours, at room temperature). Membranes were developed using Amersham ECL Prime Western Blotting Detection Reagent (GE Healthcare). The relative abundance of studied proteins was determined with densitometry. β-actin (mouse monoclonal, 1:15,000, for 45 minutes, at room temperature, Abcam) was used for normalization purposes.

Immunofluorescent Labeling and Confocal Microscopy

Mice were transcardially perfused with 1× heparin containing PBS, then brains were removed and hemisected. The left hemispheres were fixed overnight in 4% paraformaldehyde, then were cryoprotected in a series of graded sucrose solutions (10%, 20%, and 30% overnight) and frozen in Cryo-Gel (Electron Microscopy Sciences, Hatfield, PA). Coronal sections of 35 µm were cut through the hippocampus and stored free-floating in cryopreservative solution (25% glycerol, 25% ethylene glycol, 25% 0.2M phosphate buffer, 25% distilled water) at –20°C. Selected sections were ~1.6 mm caudal to Bregma, representing the more rostral hippocampus. After washing (3 × 5 minutes with TBS then 3 × 5 minutes with 1× TBS+0.25% TritonX-100), sections were treated with 1% of sodium-borohydride solution for 5 minutes. After a second washing step (3 × 5 minutes with distilled water plus 3 × 5 minutes with 1× TBS) and blocking in 5% BSA/TBS (with 0.5% Triton X-100, 0.3 M glycin and 1% fish gelatin; for 3 hours), sections were immunostained using primary antibodies overnifght at 4°C. The following primary antibodies were used: goat anti-mouse IgG (1:100, FITC conjugated; Cat N: 005-090-003, Jackson Immuno Research, West Grove, PA) to label extravasated IgG, rabbit anti-mouse Iba1 (1:50, unconjugated; Cat N: 019-19741, Wako, Richmond, VA) to label microglia and rabbit anti-mouse CD68 (1:100, unconjugated; Cat N: ab125212, Abcam, Cambridge, MA) to label activated microglia. The following secondary antibodies were used: Alexa Fluor 647- and Alexa Fluor 568-labeled goat anti-rabbit IgG, (1:1,000, Cat N: 4414, Cell Signaling, Danvers, MA) and goat anti-rat IgG, (1:1,000, Cat N: A11077, Molecular Probes, Grand Island, NY). Sections were washed for 3 × 5 minutes with TBS then 3 × 5 minutes with 1× TBS+0.25% TritonX-100. For nuclear counterstaining, Hoechst 33342 (Life Technologies, Grand Island, NY) was used. Then the sections were transferred to slides and cover-slipped. Confocal images were captured using a Leica SP2 MP confocal laser scanning microscope. Immunofluorescent labeling for Iba1 and CD68 was used to identify microglia and activated microglia, respectively. The relative numbers of Iba1-positive microglia and CD68-positive activated microglia per region of interest in the hippocampus were calculated. In each animal, four randomly selected fields from the hippocampus were analyzed in 6 nonadjacent sections. Six animals per group were analyzed.

Electrophysiological Studies for Synaptic Function and LTP

To assess how Nrf2 deficiency and obesity affect synaptic function, extracellular recordings were performed from acute hippocampal slices with an adapted protocol (11,35,36). Briefly, horizontal hippocampal slices of 325 µm thickness from mice in each cohort were prepared in ice cold solution containing (in mmol/L) sucrose 110, NaCl 60, KCl 3, NaH_2PO_4 1.25, $NaHCO_3$ 28, sodium ascorbate acid 0.6, glucose 5, $MgCl_2$ 7, $CaCl_2$ 0.5 using a HM650V vibrating microtome (Thermo Scientific). Slices were then transferred to a holding chamber (Scientific Designs, Inc.) which contained oxygenated artificial cerebrospinal fluid (aCSF) of the following composition (in mmol/L) NaCl 126, KCl 2.5, NaH_2PO_4 1.25, $MgCl_2$ 2, $CaCl_2$ 2, $NaHCO_3$ 26, glucose 10, pyruvic acid 2, ascorbic acid 0.4. Slices were left to recover for at least 60 min at room temperature prior to recording in a brain slice chamber (Automate Scientific Inc., CA). Slices from the treatment and control groups were positioned on P5002A multi-electrode arrays (Alpha MED Scientific Inc, Japan) and perfused with aCSF at a rate of 2 ml/min, equilibrated with 95% O_2 and 5% CO_2 at 32°C. fEPSPs were invoked through stimulation of the Schaffer collaterals (0.2 msec biphasic pulse) and obtained from the CA1 region of the hippocampus. Threshold for evoking fEPSPs was determined and the stimulus was increased incrementally (5–100 µA) until the maximum amplitude of the fEPSP was reached. All other stimulation paradigms were induced at the same half-maximal stimulus strength, defined as 50% of the stimulus used to produce the maximum fEPSP amplitude, as determined for each individual slice. After a stable baseline recording of 15 minutes was established, LTP was induced using high-frequency stimulation, which consisted of 100 pulses at 100 Hz applied with half-minute intervals. fEPSPs were monitored every 30 seconds for 60 minutes following high-frequency stimulation and were recorded with MED-64 system and Mobius software (Alpha MED Scientific Inc). Potentiation was calculated as the percent increase of the mean fEPSP descending slope following high-frequency stimulation and normalized to the mean fEPSP descending slope of baseline recordings.

Table 1. Effects of HFD on body mass and various serum biomarkers and metabolic parameters in Wt and Nrf2$^{-/-}$ mice

	Wt (SD)	Wt (HFD)	Nrf2$^{-/-}$ (SD)	Nrf2$^{-/-}$ (HFD)
Glucose (mmol/L, fasted)	4.8 ± 0.4	5.0 ± 0.4	2.5 ± 0.1*	2.7 ± 0.2*,**
Glucose (mmol/L, fed)	6.9 ± 0.4	9.4 ± 0.9	5.4 ± 0.5	7.0 ± 0.6
Total cholesterol (mmol/L)	2.4 ± 0.2	4.4 ± 0.6	2.0 ± 0.1	3.0 ± 0.2
Total triglycerides (mmol/L)	0.7 ± 0.1	0.8 ± 0.1	0.7 ± 0.1	0.7 ± 0.1
IL-6 (pg/mL)	43 ± 8	149 ± 25*	40 ± 3	143 ± 67*,***
MCP-1 (pg/mL)	24 ± 2	22 ± 1	29 ± 3	52 ± 11*,**,***
KC (pg/mL)	117 ± 21	267 ± 44*	131 ± 25	658 ± 290*,***
G-CSF (pg/mL)	529 ± 110	1,973 ± 424*	527 ± 83	1,363 ± 306*,***
TNFα (pg/mL)	20 ± 2	23 ± 1	23 ± 2	37 ± 8*,**,***
IL-1β (pg/mL)	18 ± 2	19 ± 1	18 ± 1	34 ± 9*,**,***
IL-12 (pg/mL)	22 ± 2	25 ± 2	32 ± 8	43 ± 13
RANTES (pg/mL)	60 ± 10	58 ± 8	67 ± 15	72 ± 15
MIP-2 (pg/mL)	26 ± 2	30 ± 3	25 ± 2	30 ± 3
MIP-1α (pg/mL)	23 ± 2	26 ± 2	23 ± 1	32 ± 3*,***
MIP-1β (pg/mL)	28 ± 4	36 ± 4	37 ± 5	80 ± 22*,**,***
IL-10 (pg/mL)	38 ± 4	34 ± 3	47 ± 11	44 ± 3
IL-17 (pg/mL)	40 ± 7	105 ± 20*	64 ± 13	197 ± 71*,***
IP-10 (pg/mL)	1,179 ± 213	1,462 ± 271	1,062 ± 184	1,428 ± 240
IL-5 (pg/mL)	35 ± 8	25 ± 2	36 ± 4	22 ± 3
GM-CSF (pg/mL)	25 ± 2	26 ± 3	30 ± 5	155 ± 93

Note: Data are mean ± SEM (n = 4–20 for each data point).

*p < .05 vs Nrf2$^{+/+}$ (SD), **p < .05 vs. Nrf2$^{+/+}$ (HFD), ***p < .05 vs Nrf2$^{-/-}$ (SD); one-way ANOVA; G-CSF = Granulocyte-colony stimulating factor; HFD = High-fat diet; KC = Keratinocyte-derived chemokine; MIP-2 = Macrophage inflammatory protein 2; RANTES = Regulated on activation, normal T cell expressed and secreted; Wt = Wild type.

Data Analysis

Gene expression data were normalized to the respective control mean values and are expressed as fold changes. Data were analyzed by one-way analysis of variance (ANOVA) followed by Tukey's post-hoc test. A p value less than .05 was considered statistically significant. Data are expressed as mean ± SEM.

Results

Effect of a High-Fat Diet on Serum Biomarkers

We compared male Nrf2$^{+/+}$ and Nrf2$^{-/-}$ mice after 5 months of the HFD. Blood glucose levels and serum triglyceride, cholesterol, and inflammatory cytokines levels are shown in Table 1.

Expression of Antioxidant Enzymes in Nrf2$^{-/-}$ Mice

Nrf2 deficiency was associated with decreased cerebral mRNA and/or protein expression of Nrf2/ARE (antioxidant response element)-driven antioxidant enzymes (Figure 1A and B), whereas expression of antioxidant enzymes, whose promoter does not contain an ARE motif was unaffected (Figure 1C). HFD did not result in significant changes in antioxidant gene expression in either group (Figure 1A–C).

Increased Oxidative Stress and Senescence in HFD-fed Nrf2$^{-/-}$ Mice

Although HFD tended to increase protein carbonyl content in the brains of Nrf2$^{+/+}$ mice (Figure 1D), this difference did not reach statistical significance. HFD-induced oxidative stress was more severe in Nrf2$^{-/-}$ mice, as shown by the significantly greater level of protein carbonyl content in the brains of HFD-fed Nrf2$^{-/-}$ mice as compared to that in HFD-fed Nrf2$^{+/+}$ mice (Figure 1D). HFD-induced oxidative stress was shown to promote cellular senescence in multiple tissues (37,38). We found that exacerbation of HFD-induced oxidative stress in Nrf2$^{-/-}$ mice was associated with upregulation of the senescence marker p16^{INK4A} (*Cdk2na*; Figure 1E) in the brain.

Nrf2 Deficiency Exacerbates Obesity-Induced Neurovascular Uncoupling

In Nrf2$^{+/+}$ mice feeding, a HFD resulted in significantly decreased whisker stimulation induced CBF responses in the contralateral whisker barrel cortex, confirming our previous findings (8) (representative laser Doppler CBF tracings are shown in Figure 2A, summary data are shown in Figure 2B). Neurovascular coupling responses were also decreased in SD-fed Nrf2$^{-/-}$ mice (Figure 2). We found that Nrf2 deficiency exacerbated the deleterious effects of obesity, quasi-abolishing neurovascular coupling responses (Figure 2A and B). Nrf2 deficiency and/or HFD feeding could reduce functional hyperemia by impairing neural activity evoked by whisker pad stimulation. To examine this possibility, we assessed the effects of Nrf2 deficiency and/or HFD feeding by recording evoked neural activity. We found that the amplitude of the somatosensory field potentials produced by activation of the whisker pad do not differ between control and Nrf2-deficient mice and are also unaffected by HFD feeding (data not shown). Therefore, interaction of Nrf2 deficiency and obesity is unlikely to contribute to impaired functional hyperemia by modulating the neural activity evoked by whisker stimulation. Changes in mRNA expression of genes relevant for neurovascular dysfunction are shown in Figure 2C.

Nrf2 Deficiency Exacerbates Obesity-Induced BBB Disruption

Using extravasated plasma-derived IgG as a marker for increased hippocampal cerebromicrovascular permeability, we tested the hypothesis that increased obesity-induced oxidative stress in Nrf2 deficiency is associated with an exacerbated BBB disruption. Western blot studies in hippocampal lysates demonstrated very low levels of IgG both in SD-fed and HFD-fed Nrf2$^{+/+}$ mice (Figure 3A and B).

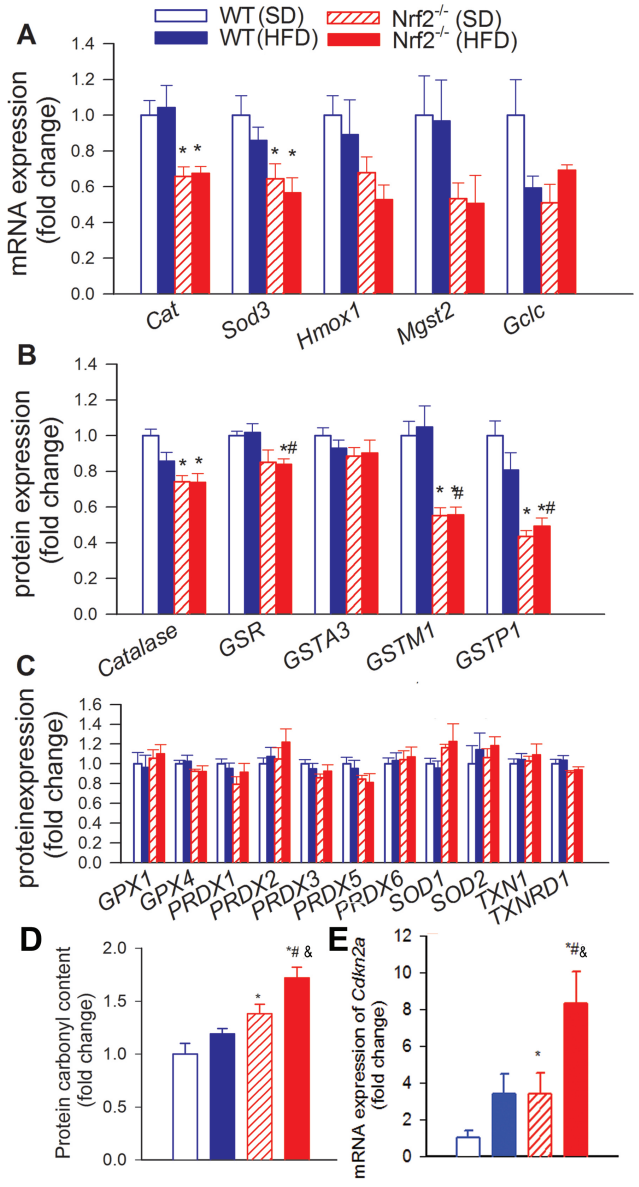

Figure 1. Nrf2 deficiency exacerbates obesity-induced oxidative stress. Effects of Nrf2 deficiency and obesity on expression of known Nrf2 target genes at the mRNA (**A**; quantitative polymerase chain reaction data) and protein (**B**; quantitative proteomics/selective reaction monitoring [SRM]) level. (**C**) Effects of Nrf2 deficiency and obesity on protein expression of antioxidant enzymes, whose promoter is not under the control of the Nrf2/ARE system (quantitative proteomics/SRM). (**D**) Nrf2 deficiency exacerbates high-fat diet (HFD)-induced oxidative stress. Note the significant increases in protein carbonyl content (a marker of oxidative stress) in brain samples from HFD-fed Nrf2$^{-/-}$ mice, which associates with up-regulation of *Cdkn2a* (p16INK4A; panel **E**), a marker of increased stress-induced cellular senescence. Data are mean ± SEM (n = 5–6 for each data point). $^{*}p < .05$ vs Wt (SD), $^{\#}p < .05$ vs Wt (HFD), $^{\&}p < .05$ vs Nrf2$^{-/-}$ (SD) (one-way analysis of variance, Tukey's post hoc test).

There was no significant IgG leakage in SD-fed Nrf2$^{-/-}$ mice, whereas IgG content in the hippocampus of HFD-fed Nrf2$^{-/-}$ mice was significantly increased (Figure 3A and B).

Nrf2 Deficiency Exacerbates Obesity-Induced Neuroinflammation in the Hippocampus

Previous studies suggest that leakage of plasma-derived factors through the damaged BBB has the potential to induce neuroinflammation by activating microglia (7). We found that in the hippocampi of control mice the number of activated CD68+ microglia was low (Figure 3C–E). In the present cohort of Nrf2$^{+/+}$ mice HFD feeding did not alter significantly the number of activated microglia in the hippocampi. Nrf2 deficiency *per se* was also not associated with significant changes in microglia activation. In contrast, in the hippocampi of Nrf2$^{-/-}$ mice, obesity-induced oxidative stress and BBB disruption was associated with exacerbated neuroinflammation as indicated by the increased number of CD68+ activated microglia (Figure 3E). Nrf2 deficiency and obesity did not alter the total number of microglia in the hippocampus (Figure 3D). Sustained activation of microglia in the brain of obese Nrf2 deficient mice was associated with an increased expression of several proinflammatory cytokines and chemokines and other microglia activation-related factors (Figure 3F) in the hippocampi.

Effects of Nrf2 Deficiency and Obesity on Hippocampal Expression of APP and Genes Involved in APP-Dependent Signaling, Aβ Processing and Tauopathy

As observed in Supplementary Table S2, neither obesity nor Nrf2 deficiency alone affected cerebral expression of APP, whose proteolysis generates β-amyloid (Aβ), the main component of amyloid plaques. Importantly, HFD-fed Nrf2$^{-/-}$ mice exhibited significant increases in APP expression. The effects of Nrf2 deficiency and obesity on hippocampal expression of other genes involved in APP-dependent signaling, Aβ processing and tauopathy are shown in Supplementary Table 1. Interestingly, although we did not observe upregulation of either amyloid processing secretases, HFD significantly increased presenilin enhancer 2 levels, which is known to enhance gamma-secretase activity and promote formation of amyloid plaques (39,40).

Effects of Nrf2 Deficiency and Obesity on Synaptic Plasticity

Increased oxidative stress and neuroinflammation has been linked to impairment of long-term potentiation, which is thought to promote impairment of memory and learning. In order to characterize the effects of Nrf2 deficiency and obesity on synaptic function, we measured EPSP in the CA1 of hippocampi in response to electrical stimulation of the Schaffer collaterals pathway (with 5 µA steps increased up to 100 µA). Original recordings showing field EPSPs in the CA1 in response to the stimulation of the Schaffer collaterals in each group are shown in Figure 4A. We found that each group of mice exhibited normal basal synaptic properties. In particular, the ratio of evoked responses to the presynaptic fiber volley was similar in the experimental groups, showing that obesity does not affect neuronal EPSP. Following a 100Hz tetanic stimulation, the slope of field EPSP in the CA1 increased significantly less in the SD-fed Nrf2$^{-/-}$ group as compared to the SD-fed Nrf2$^{+/+}$ controls during the 60 minutes experimental period (Figure 4B). In the Nrf2$^{+/+}$ group, obesity also tended to decrease LTP, however, these differences did not reach statistical significance. In the hippocampi of Nrf2-deficient mice, obesity-induced impairment of LTP was exacerbated (Figure 4B).

Nrf2 Deficiency Exacerbates Obesity-Induced Cognitive Impairment

We tested the performance of the mice in the novel object recognition test. We found no significant difference in the time that mice from each group spent exploring the two identical objects placed at the opposite

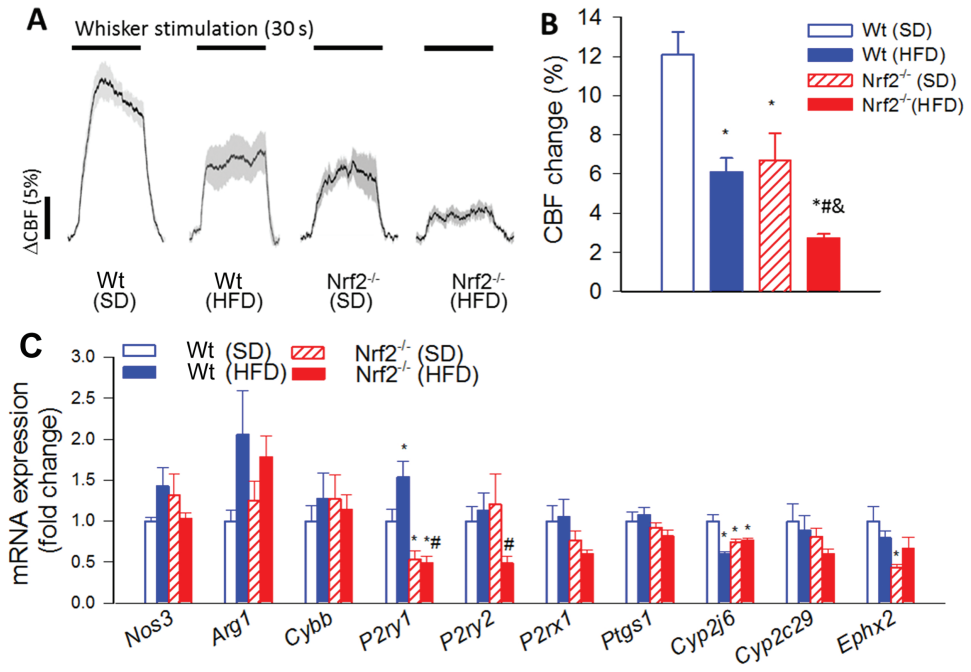

Figure 2. Nrf2 deficiency exacerbates obesity-induced neurovascular uncoupling. (**A**) Representative traces of cerebral blood flow (CBF) measured with a laser Doppler probe above the whisker barrel cortex during contralateral whisker stimulation (30 seconds, 5 Hz) in wild type (Wt) and Nrf2$^{-/-}$ mice fed a high-fat diet (HFD) or standard diet (SD). Panel **B** depicts the summary data of the effect of HFD-induced obesity on CBF responses to whisker-stimulation in Wt and Nrf2$^{-/-}$ mice. (**C**) Quantitative polymerase chain reaction data showing HFD-induced changes in mRNA expression of genes relevant for the mediation of neurovascular coupling responses by NO, purinergic signaling and eicosanoid gliotransmitters in the cortices of Wt and Nrf2$^{-/-}$ mice. Data are mean ± SEM (n = 5–10 in each group). *p < .05 vs Wt (SD), $^{\#}p$ < .05 vs Wt (HFD), $^{\&}p$ < .05 vs Nrf2$^{-/-}$ (SD) (one-way analysis of variance, Tukey's post hoc test).

ends of the arena during the acquisition phase, confirming that the location of the objects did not affect the exploration behavior of mice (11,26). In the trial phase with two different objects (one novel, the other familiar), control mice explored the novel object for a significantly longer time period, indicating their memory for the familiar object (Figure 4D). Among the four groups obese Nrf2$^{-/-}$ mice exhibited the lowest Recognition Index, which was statistically different from the control values. This result is consistent with their impaired hippocampal- and cortical-dependent recognition memory (Figure 4D).

Discussion

This is the first study to demonstrate exacerbation of obesity-induced oxidative stress, neurovascular uncoupling, BBB disruption, and neuroinflammation in a mouse model of genetic Nrf2 deficiency that recapitulates critical aspects of the cerebromicrovascular aging phenotype.

Previous studies provide ample evidence that the Nrf2/Antioxidant Response Element (ARE) pathway has a critical role in microvascular protection (15–21,41–43), especially under pathophysiological conditions associated with increased production of ROS. High-fat diet-induced obesity in aged rodents exerts deleterious effects on neurovascular coupling responses, at least in part, due to an increased production of ROS in the microvascular endothelium (8). Here, we demonstrate that Nrf2 deficiency exacerbates obesity-induced oxidative stress (Figure 1) and neurovascular impairment (Figure 2), mimicking the aging phenotype (8). We predict that significant impairment of a key homeostatic mechanism matching energy supply with the needs of active neuronal tissue likely has a profound negative effect on brain function in elderly obese patients. This prediction is supported by the observations that cognitive function is significantly impaired in obese Nrf2$^{-/-}$ mice and that pharmacological inhibition of neurovascular coupling responses in control mice is associated with a similar degree of cognitive impairment (11). Aging in both rodents and primates is associated with Nrf2 dysfunction in the vasculature (20,21). Recently, we demonstrated that treatment with a pharmacological activator of Nrf2 (3,5,4′-trihydroxy-trans-stilbene/resveratrol (17)) significantly improves neurovascular coupling responses in aged mice by restoring cerebromicrovascular endothelial function (29), which associates with cognitive improvement (44). We have compelling data that resveratrol treatment also rescues endothelial function in both larger arteries and peripheral microvessels in aged high-fat diet-fed mice in a Nrf2-dependent manner (17,18,23). Resveratrol was also shown to exert significant vasoprotective effects in HFD-fed primates as well (10,45). On the basis of the aforementioned studies, we predict that treatment with Nrf2 activators may rescue cerebromicrovascular function and thereby neurovascular coupling responses in obese subjects as well.

The results of this study show that high-fat diet-induced obesity in Nrf2 deficient mice promotes significant BBB disruption (Figure 3). The mechanisms of obesity-related BBB disruption are likely multifaceted and may involve increased endothelial oxidative stress (7), which is known to be exacerbated by Nrf2 deficiency (17,18). Obesity is known to promote low-grade systemic inflammation, at least in part, by upregulating production of inflammatory cytokines by the adipose tissue (9). Circulating inflammatory cytokines, derived from adipose tissue, readily reach the cerebral microcirculation impairing the barrier function of cerebromicrovascular endothelial cells. Importantly, Nrf2 activity is known to limit cytokine-induced endothelial effects. Our current study provides evidence that through the damaged BBB in obese Nrf2-deficient

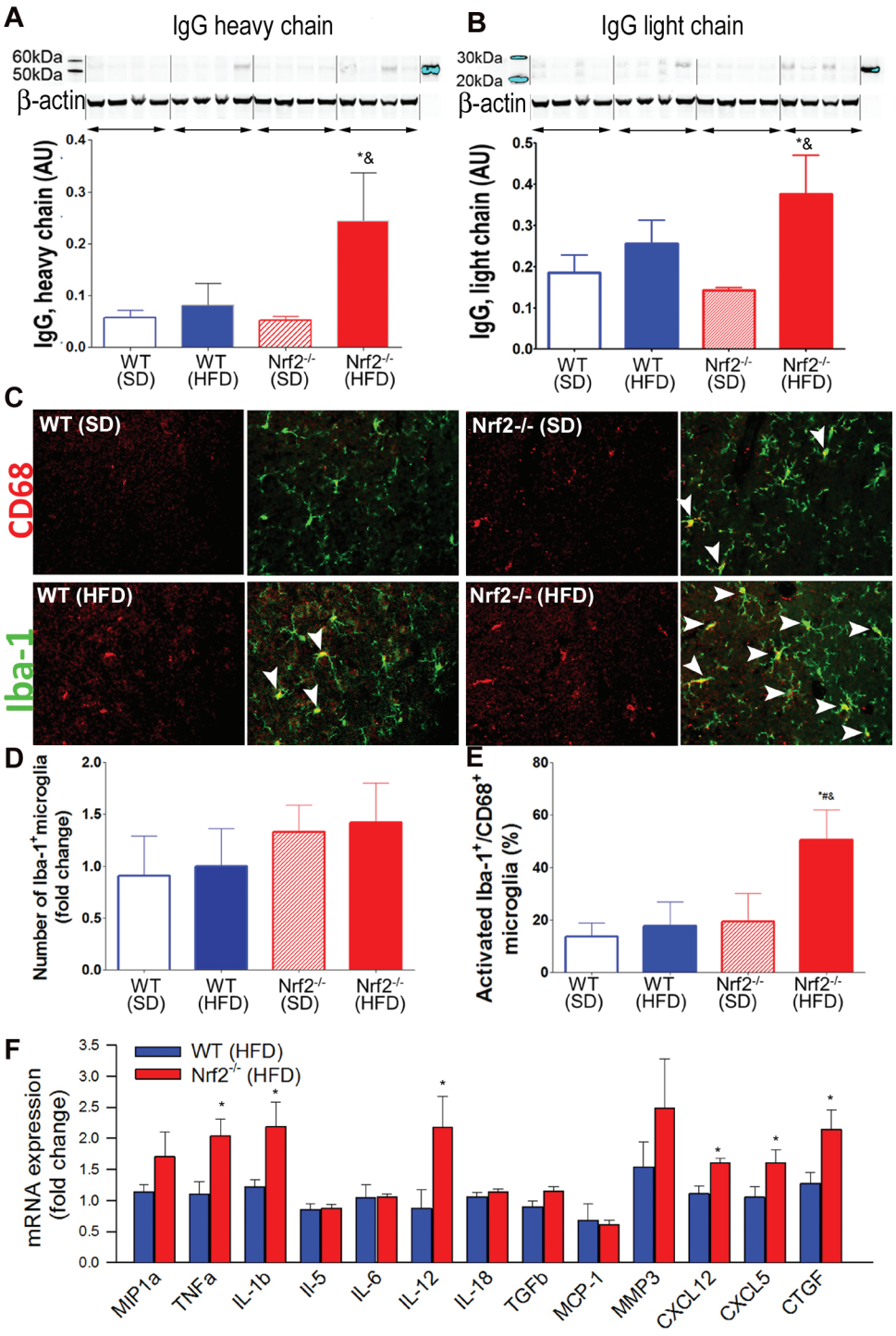

Figure 3. Nrf2 deficiency exacerbates obesity-induced disruption of the blood-brain barrier and promotes neuroinflammation. (**A,B**) Obesity and Nrf2 deficiency-induced changes in IgG content in the hippocampus of mice. Upper panel: original Western blot showing IgG heavy chain (**A**) and light chain (**B**) content in the hippocampi. β-actin was used as a loading control. Bar graphs are summary densitometric values. Data are mean ± SEM. $^{*}p < .05$ vs Wt (SD), $^{\#}p < .05$ vs Wt (HFD); $^{\&}p < .05$ vs Nrf2$^{-/-}$ (SD). (**C**) Confocal images showing CD68-positive (red fluorescence, arrowheads) activated microglia in the hippocampi from wild-type SD-fed), wild-type HFD-fed, Nrf2$^{-/-}$ SD-fed, and Nrf2$^{-/-}$ HFD-fed animals. Green fluorescence: Iba-1 microglia marker. Bar graphs are summary data for relative changes in total Iba-1-positive microglia (**D**) and CD68^{+}/Iba-1^{+}-activated microglia (**E**). Data are mean ± SEM. $^{*}p < .05$ vs Wt (SD), $^{\#}p < .05$ vs Wt (HFD); $^{\&}p < .05$ vs Nrf2$^{-/-}$ (SD). (**F**) Quantitative polymerase chain reaction data showing HFD-induced changes in mRNA expression of proinflammatory cytokines and chemokines and other microglia activation-related factors in the hippocampi of Wt and Nrf2$^{-/-}$ mice. Data are mean ± SEM. $^{*}p < .05$.

mice plasma constituents (e.g., IgG) enter the brain parenchyma (Figure 3), mimicking the aging phenotype (7). This observation is important as plasma-derived factors exert multifaceted effects on neuronal function, including the induction of neuroinflammation (13,46,47). There is strong evidence that plasma-derived IgG is a particularly potent stimulus for microglia activation in the brain

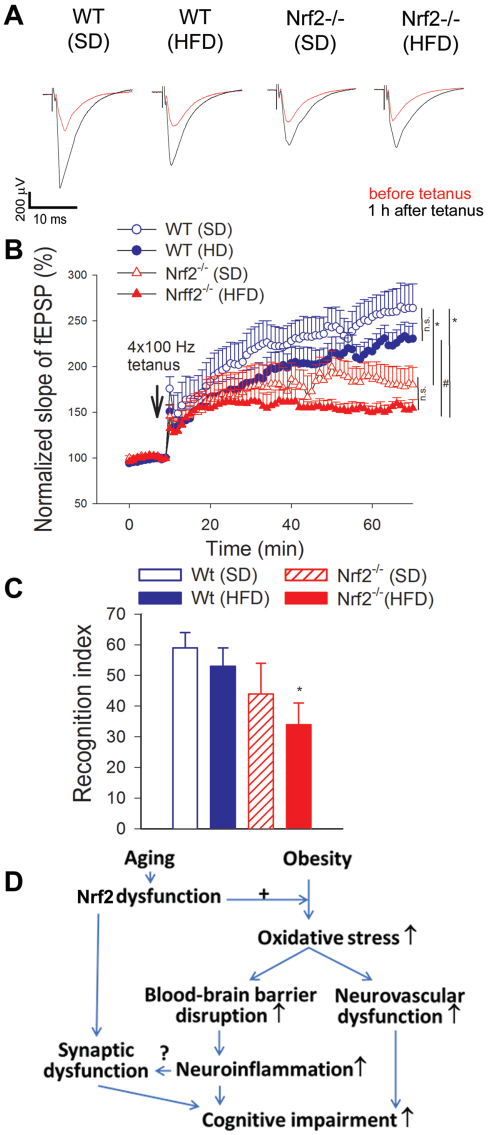

Figure 4. (**A**) Original recordings showing the effects of Nrf2 deficiency and high-fat diet (HFD)-induced obesity on field excitatory postsynaptic potential (EPSP) in the CA1 in response to the stimulation of the Schaffer collaterals on hippocampal brain slices before (10 minutes) and 1 hour after (70 minutes) 4 × 100 Hz tetanus. (**B**) Long-term potentiation shown as change of field EPSP (fEPSP) slope following a 4 × 100 Hz (1 second) tetanic stimulus in the CA1 of the hippocampus. Data are normalized to baseline responses and depicted as mean ± SEM (n = 8–12 for each data point); *$p < .05$ vs Wt (SD), $^{\#}p < .05$ vs Wt (HFD) during the last 5 minutes of the recording. (**C**) The novel object recognition task test used to evaluate recognition memory in mice. The Recognition Index (representing the time spent investigating the novel object relative to the total object investigation) was used as the main index of retention. Data are mean ± SEM. *$p < .05$ vs Wt (SD). (**D**) Proposed scheme depicting the likely role of age-related Nrf2 dysfunction in exacerbation of obesity-induced oxidative stress, BBB disruption, neuroinflammation, neurovascular dysfunction, and synaptic dysfunction, all of which contribute to cognitive impairment in obese elderly subjects.

(7). Other plasma constituents that likely contribute to microglia activation upon BBB disruption include thrombin, fibrinogen, and circulating inflammatory cytokines. Here, we provide evidence that in obese Nrf2-deficient mice, similar to obese aged mice (7), BBB disruption and increased extravasation of plasma constituents are associated with an exacerbated neuroinflammatory response as shown by the increased number of activated microglia and upregulation of inflammatory mediators (e.g., IL-1β (48)) in the hippocampus. On the basis of the present and previous findings we propose that age-related microvascular Nrf2 dysfunction likely contributes to exacerbation of obesity-induced BBB disruption and neuroinflammation in aged mice (7).

Clinical studies demonstrate that increased inflammation predicts cognitive decline. Results of preclinical studies support this concept by showing that microglia-derived proinflammatory cytokines, chemokines, proteases (MMPs), and reactive oxygen species promote neuronal dysfunction, including impairment of synaptic function. To determine the functional consequences of exacerbated neuroinflammation in obese Nrf2-deficient mice, we studied LTP (an increase in synaptic strength), which plays an important role in the establishment and storage of stable long-term memories in the hippocampus. We found that HFD-induced obesity tended to decrease LTP in the hippocampus, confirming previous findings (49). In obese Nrf2-deficient mice, LTP was substantially reduced, which, together with neurovascular uncoupling, likely contributes to impaired cognitive performance (Figure 4A–C). Interestingly, Nrf2 deficiency itself also appears to decrease LTP, supporting the concept that Nrf2 deficiency exerts multifaceted adverse neuronal effects. For example, recent studies show that Nrf2 ortholog SKN-1 regulates synaptic transmission in *C. elegans* (50). Further, in mice, intrahippocampal injections of a lentiviral vector expressing Nrf2 improve spatial learning (51). The exact mechanisms linking Nrf2 activation to synaptic strength in mice are not understood and should be elucidated in future studies.

Epidemiological studies provide evidence that in addition to the established association of obesity with vascular cognitive impairment, there is a direct relationship between obesity and pathogenesis of AD (reviewed in ref. (52)). In particular, BBB disruption, increased inflammatory status and oxidative stress are thought to contribute to the pathogenesis of AD, via mechanisms that include dysregulation of AD-related gene expression (7,26). To determine whether in Nrf2-deficient mice exacerbated obesity-induced cerebromicrovascular alterations and neuroinflammation were sufficient to trigger early processes involved in the pathogenesis of Alzheimer's disease, we assessed hippocampal expression of genes involved in regulation of the cellular APP-dependent signaling pathways, beta-amyloid generation and processing and the pathogenesis of tauopathy. Importantly, obesity in Nrf2-deficient mice resulted in significant alterations in amyloidogenic gene expression, including upregulation of cerebral expression of APP, whose proteolysis generates Aβ, the main component of amyloid plaques (Supplementary Table S1). This finding is consistent with the results of previous studies showing that increased oxidative stress induces APP expression and that Nrf2 deficiency (53) and HFD-induced obesity (54) exacerbate AD pathologies in genetic mouse models.

Collectively, our findings provide evidence that Nrf2-driven free radical detoxification pathways have an important role in neurovascular protection in obesity (Figure 4D). We find that Nrf2 dysfunction compromises cerebromicrovascular and brain health, by exacerbating obesity-induced neurovascular uncoupling, BBB disruption, neuroinflammation, and synaptic dysfunction, promoting cognitive impairment. We propose that pathological conditions that impair cellular Nrf2 activity, such as advanced aging (15,19–21,42), render the cerebral microvasculature vulnerable to the deleterious effects of obesity, which likely plays a critical role in the augmented pathogenesis of VCI and AD. Based on our present and previous

findings, there is a clear opportunity for pharmacological intervention to facilitate induction of Nrf2-driven homeostatic pathways by pharmacological treatments for the prevention of cognitive impairment in obese elderly patients.

Supplementary Material

Supplementary data is available at *The Journals of Gerontology, Series A: Biological Sciences and Medical Sciences* online.

Funding

This work was supported by grants from the American Heart Association (S.T., M.N.V.-A., Z.T., Z.U., and A.C.), the Oklahoma Center for the Advancement of Science and Technology (to A.C., A.Y., F.D., and Z.U.), the National Center for Complementary and Alternative Medicine (R01-AT006526 to Z.U.), the National Institute on Aging (R01-AG047879; R01-AG055395; R01-AG038747; P30 AG050911), the National Institute of Neurological Disorders and Stroke (NINDS; R01-NS056218 to A.C.), the National Heart, Lung and Blood Institute (R01-HL132553), the Oklahoma Shared Clinical and Translational Resources (OSCTR) program funded by the National Institute of General Medical Sciences (GM104938, to A.Y., P20GM104934 to F.D.), the National Eye Institute (R01-EY019494, to M.H.E. and core grant P30-EY021725), the Oklahoma IDeA Network for Biomedical Research Excellence (to A.C. and F.D.), the Presbyterian Health Foundation (to Z.U., A.C., A.Y., and F.D.), the Research to Prevent Blindness foundation (to the Dean McGee Eye Institute), and the Intramural Research Program of NIH (to R.D.C.). The authors acknowledge the support from the NIA-funded Geroscience Training Program in Oklahoma (T32AG052363).

Conflict of Interest

R.D.C. serves as Editor-in-Chief of the Journal of Gerontology - Biological Sciences. Z.U. serves as Associate Editor.

References

1. Wolf PA, Beiser A, Elias MF, Au R, Vasan RS, Seshadri S. Relation of obesity to cognitive function: importance of central obesity and synergistic influence of concomitant hypertension. The Framingham Heart Study. *Curr Alzheimer Res*. 2007;4:111–116.
2. Gustafson DR, Karlsson C, Skoog I, Rosengren L, Lissner L, Blennow K. Mid-life adiposity factors relate to blood-brain barrier integrity in late life. *J Intern Med*. 2007;262:643–650. doi:10.1111/j.1365-2796.2007.01869.x
3. Beydoun MA, Beydoun HA, Wang Y. Obesity and central obesity as risk factors for incident dementia and its subtypes: a systematic review and meta-analysis. *Obes Rev*. 2008;9:204–218. doi:10.1111/j.1467-789X.2008.00473.x
4. Alosco ML, Spitznagel MB, Raz N, et al. Obesity interacts with cerebral hypoperfusion to exacerbate cognitive impairment in older adults with heart failure. *Cerebrovasc Dis Extra*. 2012;2:88–98. doi:10.1159/000343222
5. Tarantini S, Tran CH, Gordon GR, Ungvari Z, Csiszar A. Impaired neurovascular coupling in aging and Alzheimer's disease: contribution of astrocyte dysfunction and endothelial impairment to cognitive decline. *Exp Gerontol*. 2016. doi:10.1016/j.exger.2016.1011.1004
6. Toth P, Tarantini S, Csiszar A, Ungvari Z. Functional vascular contributions to cognitive impairment and dementia: mechanisms and consequences of cerebral autoregulatory dysfunction, endothelial impairment, and neurovascular uncoupling in aging. *Am J Physiol Heart Circ Physiol*. 2017;312:H1–H20. doi:10.1152/ajpheart.00581.2016
7. Tucsek Z, Toth P, Sosnowska D, et al. Obesity in aging exacerbates blood-brain barrier disruption, neuroinflammation, and oxidative stress in the mouse hippocampus: effects on expression of genes involved in beta-amyloid generation and Alzheimer's disease. *J Gerontol A Biol Sci Med Sci*. 2014;69:1212–1226. doi:10.1093/gerona/glt177
8. Tucsek Z, Toth P, Tarantini S, et al. Aging exacerbates obesity-induced cerebromicrovascular rarefaction, neurovascular uncoupling, and cognitive decline in mice. *J Gerontol A Biol Sci Med Sci*. 2014;69:1339–1352. doi:10.1093/gerona/glu080
9. Bailey-Downs LC, Tucsek Z, Toth P, et al. Aging exacerbates obesity-induced oxidative stress and inflammation in perivascular adipose tissue in mice: a paracrine mechanism contributing to vascular redox dysregulation and inflammation. *J Gerontol A Biol Sci Med Sci*. 2013;68:780–792. doi:10.1093/gerona/gls238
10. Bernier M, Wahl D, Ali A, et al. Resveratrol supplementation confers neuroprotection in cortical brain tissue of nonhuman primates fed a high-fat/sucrose diet. *Aging (Albany NY)*. 2016;8:899–916. doi:10.18632/aging.100942
11. Tarantini S, Hertelendy P, Tucsek Z, et al. Pharmacologically-induced neurovascular uncoupling is associated with cognitive impairment in mice. *J Cereb Blood Flow Metab*. 2015;35:1871–1881. doi:10.1038/jcbfm.2015.162
12. Zlokovic BV. Neurovascular pathways to neurodegeneration in Alzheimer's disease and other disorders. *Nat Rev Neurosci*. 2011;12:723–738. doi:10.1038/nrn3114nrn3114 [pii]
13. Pistell PJ, Morrison CD, Gupta S, et al. Cognitive impairment following high fat diet consumption is associated with brain inflammation. *J Neuroimmunol*. 2010;219:25–32. doi:10.1016/j.jneuroim.2009.11.010
14. Knight EM, Martins IV, Gümüsgöz S, Allan SM, Lawrence CB. High-fat diet-induced memory impairment in triple-transgenic Alzheimer's disease (3xTgAD) mice is independent of changes in amyloid and tau pathology. *Neurobiol Aging*. 2014;35:1821–1832. doi:10.1016/j.neurobiolaging.2014.02.010
15. Csiszar A, Gautam T, Sosnowska D, et al. Caloric restriction confers persistent anti-oxidative, pro-angiogenic, and anti-inflammatory effects and promotes anti-aging miRNA expression profile in cerebromicrovascular endothelial cells of aged rats. *Am J Physiol Heart Circ Physiol*. 2014;307:H292–H306. doi:10.1152/ajpheart.00307.2014
16. Pearson KJ, Lewis KN, Price NL, et al. Nrf2 mediates cancer protection but not prolongevity induced by caloric restriction. *Proc Natl Acad Sci USA*. 2008;105:2325–2330. doi:10.1073/pnas.0712162105
17. Ungvari Z, Bagi Z, Feher A, et al. Resveratrol confers endothelial protection via activation of the antioxidant transcription factor Nrf2. *Am J Physiol Heart Circ Physiol*. 2010;299:H18–H24. doi:10.1152/ajpheart.00260.2010
18. Ungvari Z, Bailey-Downs L, Gautam T, et al. Adaptive induction of NF-E2-related factor-2-driven antioxidant genes in endothelial cells in response to hyperglycemia. *Am J Physiol Heart Circ Physiol*. 2011;300:H1133–H1140. doi:10.1152/ajpheart.00402.2010
19. Csiszár A, Csiszar A, Pinto JT, et al. Resveratrol encapsulated in novel fusogenic liposomes activates Nrf2 and attenuates oxidative stress in cerebromicrovascular endothelial cells from aged rats. *J Gerontol A Biol Sci Med Sci*. 2015;70:303–313. doi:10.1093/gerona/glu029
20. Ungvari Z, Bailey-Downs L, Gautam T, et al. Age-associated vascular oxidative stress, Nrf2 dysfunction, and NF-κB activation in the nonhuman primate *Macaca mulatta*. *J Gerontol A Biol Sci Med Sci*. 2011;66:866–875. doi:10.1093/gerona/glr092
21. Ungvari Z, Bailey-Downs L, Sosnowska D, et al. Vascular oxidative stress in aging: a homeostatic failure due to dysregulation of NRF2-mediated antioxidant response. *Am J Physiol Heart Circ Physiol*. 2011;301:H363–H372. doi:10.1152/ajpheart.01134.2010
22. Morrison CD, Pistell PJ, Ingram DK, et al. High fat diet increases hippocampal oxidative stress and cognitive impairment in aged mice: implications for decreased Nrf2 signaling. *J Neurochem*. 2010;114:1581–1589. doi:10.1111/j.1471-4159.2010.06865.x
23. Pearson KJ, Baur JA, Lewis KN, et al. Resveratrol delays age-related deterioration and mimics transcriptional aspects of dietary restriction without extending life span. *Cell Metab*. 2008;8:157–168. doi:10.1016/j.cmet.2008.06.011
24. Serfilippi LM, Pallman DR, Gruebbel MM, Kern TJ, Spainhour CB. Assessment of retinal degeneration in outbred albino mice. *Comp Med*. 2004;54:69–76.

25. Bailey-Downs LC, Sosnowska D, Toth P, et al. Growth hormone and IGF-1 deficiency exacerbate high-fat diet-induced endothelial impairment in obese Lewis dwarf rats: implications for vascular aging. *J Gerontol A Biol Sci Med Sci*. 2012;67:553–564. doi:10.1093/gerona/glr197
26. Csiszar A, Tucsek Z, Toth P, et al. Synergistic effects of hypertension and aging on cognitive function and hippocampal expression of genes involved in β-amyloid generation and Alzheimer's disease. *Am J Physiol Heart Circ Physiol*. 2013;305:H1120–H1130. doi:10.1152/ajpheart.00288.2013
27. Toth P, Tarantini S, Ashpole NM, et al. IGF-1 deficiency impairs neurovascular coupling in mice: implications for cerebromicrovascular aging. *Aging Cell*. 2015;14:1034–1044. doi:10.1111/acel.12372
28. Toth P, Tarantini S, Davila A, et al. Purinergic glio-endothelial coupling during neuronal activity: role of P2Y1 receptors and eNOS in functional hyperemia in the mouse somatosensory cortex. *Am J Physiol Heart Circ Physiol*. 2015;309:H1837–H1845. doi:10.1152/ajpheart.00463.2015
29. Toth P, Tarantini S, Tucsek Z, et al. Resveratrol treatment rescues neurovascular coupling in aged mice: role of improved cerebromicrovascular endothelial function and downregulation of NADPH oxidase. *Am J Physiol Heart Circ Physiol*. 2014;306:H299–H308. doi:10.1152/ajpheart.00744.2013
30. Ungvari Z, Tarantini S, Hertelendy P, et al. Cerebromicrovascular dysfunction predicts cognitive decline and gait abnormalities in a mouse model of whole brain irradiation-induced accelerated brain senescence. *Geroscience*. 2017;39:33–42. doi:10.1007/s11357-017-9964-z
31. Lind BL, Brazhe AR, Jessen SB, Tan FC, Lauritzen MJ. Rapid stimulus-evoked astrocyte Ca2+ elevations and hemodynamic responses in mouse somatosensory cortex in vivo. *Proc Natl Acad Sci USA*. 2013;110:E4678–E4687. doi:10.1073/pnas.1310065110
32. Toth P, Csiszar A, Tucsek Z, et al. Role of 20-HETE,TRP channels & BKCa in dysregulation of pressure-induced Ca2+ signaling and myogenic constriction of cerebral arteries in aged hypertensive mice. *Am J Physiol Heart Circ Physiol*. 2013. doi:10.1152/ajpheart.00377.2013
33. Toth P, Tucsek Z, Sosnowska D, et al. Age-related autoregulatory dysfunction and cerebromicrovascular injury in mice with angiotensin II-induced hypertension. *J Cereb Blood Flow Metab*. 2013;33:1732–1742. doi:10.1038/jcbfm.2013.143
34. Kinter CS, Lundie JM, Patel H, Rindler PM, Szweda LI, Kinter M. A quantitative proteomic profile of the Nrf2-mediated antioxidant response of macrophages to oxidized LDL determined by multiplexed selected reaction monitoring. *PLoS One*. 2012;7:e50016. doi:10.1371/journal.pone.0050016
35. Oka H, Shimono K, Ogawa R, Sugihara H, Taketani M. A new planar multielectrode array for extracellular recording: application to hippocampal acute slice. *J Neurosci Methods*. 1999;93:61–67.
36. Liu CC, Tsai CW, Deak F, et al. Deficiency in LRP6-mediated Wnt signaling contributes to synaptic abnormalities and amyloid pathology in Alzheimer's disease. *Neuron*. 2014;84:63–77. doi:10.1016/j.neuron.2014.08.048
37. Escande C, Nin V, Pirtskhalava T, et al. Deleted in Breast Cancer 1 regulates cellular senescence during obesity. *Aging Cell*. 2014;13:951–953. doi:10.1111/acel.12235
38. Wang CY, Kim HH, Hiroi Y, et al. Obesity increases vascular senescence and susceptibility to ischemic injury through chronic activation of Akt and mTOR. *Sci Signal*. 2009;2:ra11. doi:10.1126/scisignal.2000143
39. Edbauer D, Winkler E, Regula JT, Pesold B, Steiner H, Haass C. Reconstitution of gamma-secretase activity. *Nat Cell Biol*. 2003;5:486–488. doi:10.1038/ncb960
40. Kimberly WT, LaVoie MJ, Ostaszewski BL, Ye W, Wolfe MS, Selkoe DJ. Gamma-secretase is a membrane protein complex comprised of presenilin, nicastrin, Aph-1, and Pen-2. *Proc Natl Acad Sci USA*. 2003;100:6382–6387. doi:10.1073/pnas.1037392100
41. Bailey-Downs LC, Mitschelen M, Sosnowska D, et al. Liver-specific knockdown of IGF-1 decreases vascular oxidative stress resistance by impairing the Nrf2-dependent antioxidant response: a novel model of vascular aging. *J Gerontol A Biol Sci Med Sci*. 2012;67:313–329. doi:10.1093/gerona/glr164
42. Csiszar A, Sosnowska D, Wang M, Lakatta EG, Sonntag WE, Ungvari Z. Age-associated proinflammatory secretory phenotype in vascular smooth muscle cells from the non-human primate Macaca mulatta: reversal by resveratrol treatment. *J Gerontol A Biol Sci Med Sci*. 2012;67: 811–820. doi:10.1093/gerona/glr228
43. Valcarcel-Ares MN, Gautam T, Warrington JP, et al. Disruption of Nrf2 signaling impairs angiogenic capacity of endothelial cells: implications for microvascular aging. *J Gerontol A Biol Sci Med Sci*. 2012;67:821–829. doi:10.1093/gerona/glr229
44. Oomen CA, Farkas E, Roman V, van der Beek EM, Luiten PG, Meerlo P. Resveratrol preserves cerebrovascular density and cognitive function in aging mice. *Front Aging Neurosci*. 2009;1:4. doi:10.3389/neuro.24.004.2009
45. Mattison JA, Wang M, Bernier M, et al. Resveratrol prevents high fat/sucrose diet-induced central arterial wall inflammation and stiffening in nonhuman primates. *Cell Metab*. 2014;20:183–190. doi:10.1016/j.cmet.2014.04.018
46. Bruce-Keller AJ, White CL, Gupta S, et al. NOX activity in brain aging: exacerbation by high fat diet. *Free Radic Biol Med*. 2010;49:22–30. doi:10.1016/j.freeradbiomed.2010.03.006
47. White CL, Pistell PJ, Purpera MN, et al. Effects of high fat diet on Morris maze performance, oxidative stress, and inflammation in rats: contributions of maternal diet. *Neurobiol Dis*. 2009;35:3–13. doi:10.1016/j.nbd.2009.04.002
48. Sobesky JL, Barrientos RM, De May HS, et al. High-fat diet consumption disrupts memory and primes elevations in hippocampal IL-1β, an effect that can be prevented with dietary reversal or IL-1 receptor antagonism. *Brain Behav Immun*. 2014;42:22–32. doi:10.1016/j.bbi.2014.06.017
49. Erion JR, Wosiski-Kuhn M, Dey A, et al. Obesity elicits interleukin 1-mediated deficits in hippocampal synaptic plasticity. *J Neurosci*. 2014;34:2618–2631. doi:10.1523/JNEUROSCI.4200-13.2014
50. Staab TA, Griffen TC, Corcoran C, Evgrafov O, Knowles JA, Sieburth D. The conserved SKN-1/Nrf2 stress response pathway regulates synaptic function in *Caenorhabditis elegans*. *PLoS Genet*. 2013;9:e1003354. doi:10.1371/journal.pgen.1003354
51. Kanninen K, Heikkinen R, Malm T, et al. Intrahippocampal injection of a lentiviral vector expressing Nrf2 improves spatial learning in a mouse model of Alzheimer's disease. *Proc Natl Acad Sci USA*. 2009;106:16505–16510. doi:10.1073/pnas.0908397106
52. Luchsinger JA. Adiposity, hyperinsulinemia, diabetes and Alzheimer's disease: an epidemiological perspective. *Eur J Pharmacol*. 2008;585:119–129. doi:10.1016/j.ejphar.2008.02.048
53. Joshi G, Gan KA, Johnson DA, Johnson JA. Increased Alzheimer's disease-like pathology in the APP/ PS1ΔE9 mouse model lacking Nrf2 through modulation of autophagy. *Neurobiol Aging*. 2015;36:664–679. doi:10.1016/j.neurobiolaging.2014.09.004
54. Vandal M, White PJ, Tremblay C, et al. Insulin reverses the high-fat diet-induced increase in brain Aβ and improves memory in an animal model of Alzheimer disease. *Diabetes*. 2014;63:4291–4301. doi:10.2337/db14-0375